CERN/ISRC/72-23

July 1972

EUROPEAN ORGANIZATION FOR NUCLEAR RESEARCH

INTERSECTING STORAGE RINGS COMMITTEE

DOUBLE ISOBAR PRODUCTION AT I.S.R.

Proposal To Study The Reaction $p+p \longrightarrow (p\pi^+\pi^-)+(p\pi^+\pi^-)$

(PAVIA-PRINCETON COLLABORATION)

CONTENTS

	Page
Abstract	
1) - Aims a) measured quantities b) statistics c) resolution	1
2) - Physics a) one-pion exchange and Pomeron exchange b) s-channel and t-channel helicity conservation c) low-t region	4
3) - Experimental Technique a) measurement outline b) ISR and SFM parameters c) trigger d) π-p separation e) monitor	7
4) - Cross-section estimates a) extrapolated total b) slope parameter	14
5) - Detection efficiency a) Montecarlo b) t-dependence	16
6) - Errors and Resolution a) angles and momenta b) multiple scattering and nuclear interactions c) mass resolution	19
7) - Background a) high multiplicity events b) neutral contamination c) beam-gas interactions	26
8) - Trigger	30
9) - Rates	32
10) - Logistics and participation	34
Appendix	36
References	37

DOUBLE-ISOBAR PRODUCTION AT I.S.R.

PROPOSAL TO STUDY THE REACTION $pp \rightarrow (p\pi^+\pi^-)+(p\pi^+\pi^-)$ AT 50 GEV CMS

(Pavia-Princeton collaboration)

ABSTRACT

We would like to study double isobar production and decay in proton-proton interactions at CERN ISR in the low-t range and concentrating on the $p\pi^+\pi^-$ decay mode. We plan to use the Split-Field Magnet in order to achieve full momentum analysis on all tracks and nominal 4C reconstruction of every event with a mass resolution of about 25 MeV. The data rate should allow a statistics of the order of 3×10^4 collected events in 120 hours of running time; the data collected should be very informative on the interaction properties of the Pomeron and on helicity conservation in diffraction processes. This experiment will be fully compatible with any of the first proposed experiments using the initial version of the SFM and its basic apparatus.

PARTICIPANTS:

PAVIA : M. Cavalli-Sforza, R. Dolfini, G. Goggi, G. Mantovani, A. Piazzoli, S. Ratti, D. Scannicchio

six additional physicists will join the experiment if approved.

PRINCETON: G.K. O' Neill, D. Coyne, at least one graduate student

1) AIMS

We propose to study the reaction:

(1) $$p+p \rightarrow (p + \pi^+ + \pi^-) + (p + \pi^+ + \pi^-)$$

at $\sim$ 50 GeV C.M.S. and at low momentum transfer with the Split Field Magnet facility at the CERN ISR. The particle systems in brackets are produced along the two beam directions with whatever value of the invariant mass.

The main interest is for the channel

(2) $$p+p \rightarrow N^* \rightarrow p\ \pi^+\ \pi^- \quad + \quad N^* \rightarrow p\ \pi^+\ \pi^-$$

where N* is a nucleon isobar with T = 1/2 and J = 1/2, i.e. N*(1470), N*(1520), N*(1688), N*(2190).

The study of double isobar production through the 3-charged particles decay mode has the advantage of a sizable branching ratio and avoids the problem of neutral particles identification and detection.

General aims of the experiment are:

a) measurement of the differential cross-section $d\sigma/dt$ for t down to the kinematical limit (figs. 1 and 2), for any combination of the above mentioned isobars;

b) determination of the decay angular distributions and study of the angular correlations;

c) collection of a total statistics of order 3.10^4 double isobars, all the kinematical quantities being measured in each event;

d) resolution of less than 25 MeV in all isobar masses.

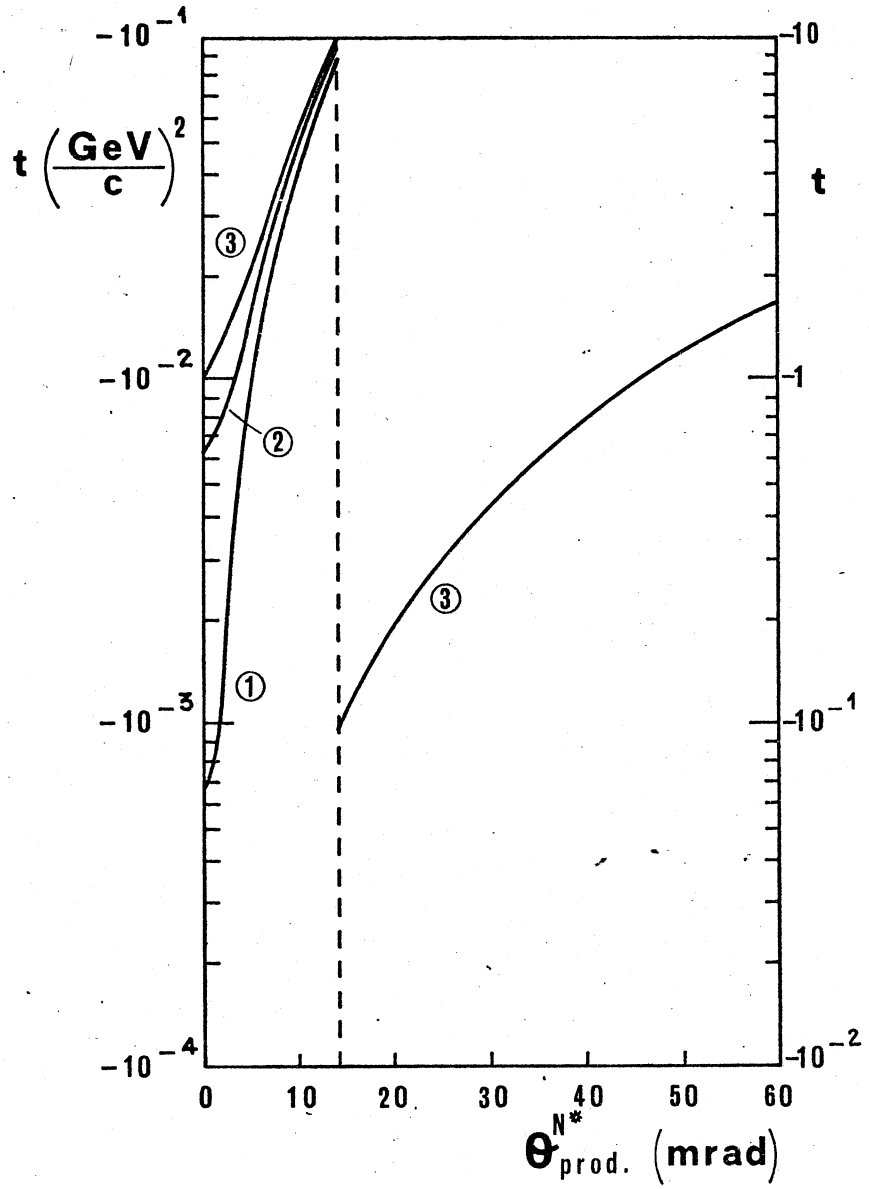

Fig. 1 – Variation of t with θ (production angle) for the following processes:

① $P + p \rightarrow N^*(1470) + N^*(1470)$

② $p + p \rightarrow N^*(1470) + N^*(2190)$

③ $p + p \rightarrow N^*(2190) + N^*(2190)$

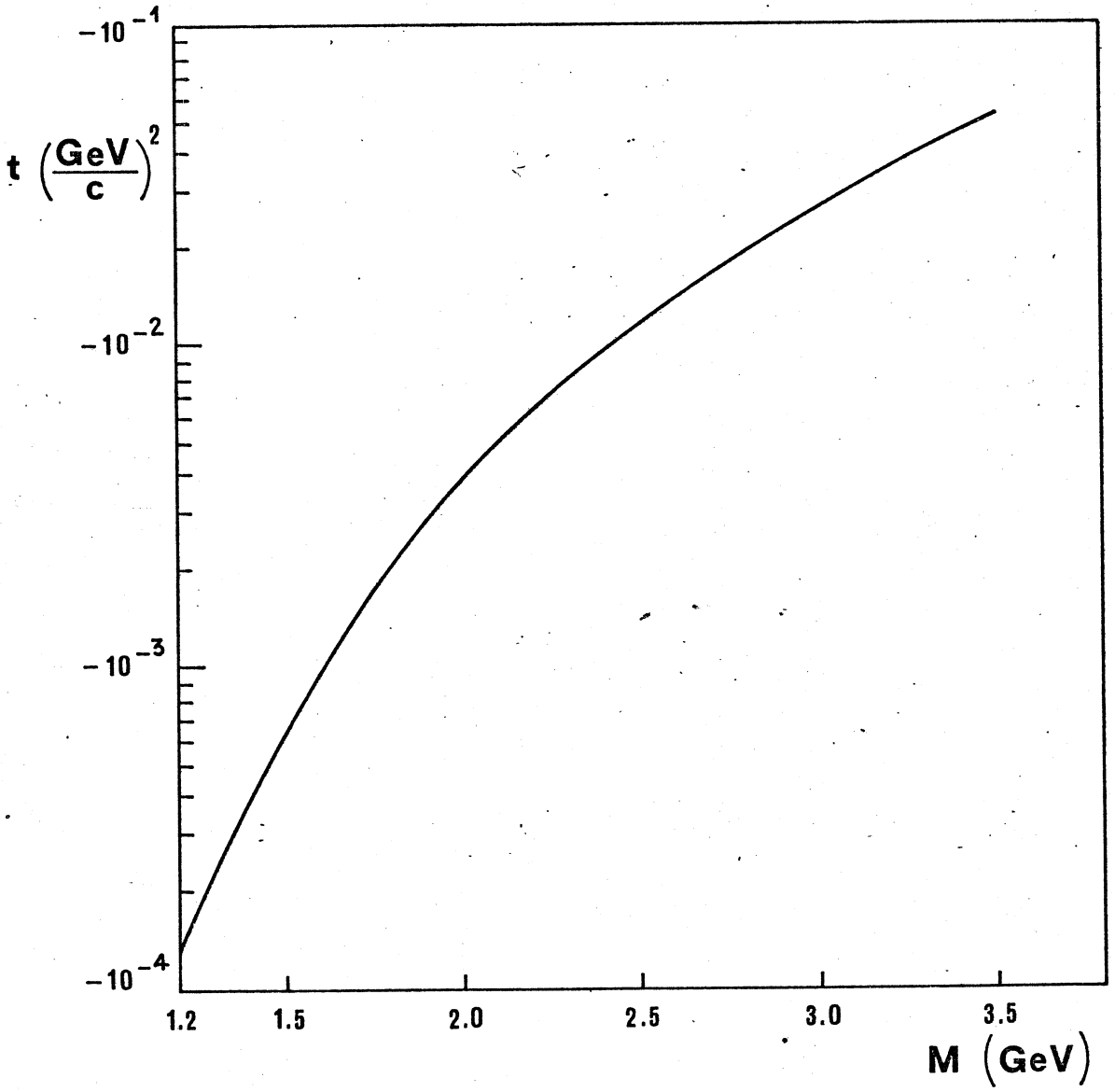

Fig. 2 - Mass dependence of minimum t-value for the production of two isobars with equal masses.

2) PHYSICS

The double production of isobars in the reaction

(3) $$p + p \longrightarrow N^* + N^*$$

has been studied in a few experiments between 4 and 10 GeV/c in bubble chambers[1-7]. In this energy interval simple isobar production is dominated by the presence of the (T = 3/2) Δ (1236). At 10 GeV, for instance, it is more than 90%. In no case is there clear experimental evidence of $N^*_{1/2} N^*_{1/2}$ production, even at higher energies where the diffraction-like reactions are supposed to dominate the isobar production[8,9]. While peripheral models (OPE plus absorption or form factors) seem to account for most of the production processes at low energy, Pomeron exchange or diffraction processes are usually assumed to dominate the high energy region, as being responsible for the flattening of the cross-sections in the asymptotic region. Recent criticisms[10] of this simplified picture revealed that pion production at presently available accelerator energies might be inconsistent with the assumption of P dominance. Böggild et al.[11] have given some indications that the isobars produced in pp collisions are dominated by exchange of spin different from zero.

The exponential behaviour of $d\sigma/dt$ is well known for $-t \gtrsim .04$ $(GeV/c)^2$; however a very narrow forward dip in isobar excitation is apparent in particle spectra at 0°[12].
The present information on the Pomeron exchange dominance in the high-energy production amplitudes is limited; this question is relevant for both the non-resonant as well as the resonant regions. For instance Satz[10] has estimated, from the branching ratio $(n\pi^+)/(p\pi^\circ)$ in 28 GeV single-isobar production, the relative importance of Pomeron exchange and isospin exchange amplitudes but all the theoretical matter is still under discussion.

The extension of these general arguments to double isobar production provides at least the following support to the experiment:

a - at extreme s-values reaction (3) should be informative about the production mechanisms. The very low t values reached in this experiment (lower than 10^{-3} $(GeV/c)^2$) should give information on the relative roles of one-pion-exchange (OPE) and Pomeron exchange. A comparison with explicit double Regge model calculations should be possible. S-channel and t-channel helicity conservation[14,15] in double diffractive processes can be tested experimentally.

b - The experimental measurement of $d\sigma/dt$ in a range of $-t$ from less than 10^{-3} $(GeV/c)^2$ to about 1.0 $(GeV/c)^2$ will allow an overlapping between a previously unaccessible t region ($-t \lesssim 10^{-2}$ $(GeV/c)^2$) and the interval already explored[16,17].

Additional features of the experiment are the following:

a - process (3) would be complementary to an already proposed experiment on single isobar production at the ISR[13]. Among the various possible inelastic sinple-channels it is one of the few which should keep a sizeable cross-section at ISR energies.

b - The process of double isobar production decaying in $p\pi^+\pi^-$ is very strong in signature and, neglecting energy conservation, allows a 3-constraint fit of the two isobar masses.

c - Detailed experimental information about this reaction in this t- region cannot readily be obtained by means of stationary-target experiments, because the decay products of an excited stationary proton would distribute over 4π in solid angle, thus preventing the unambigous identification of the two decaying excited states (over all the phase space).

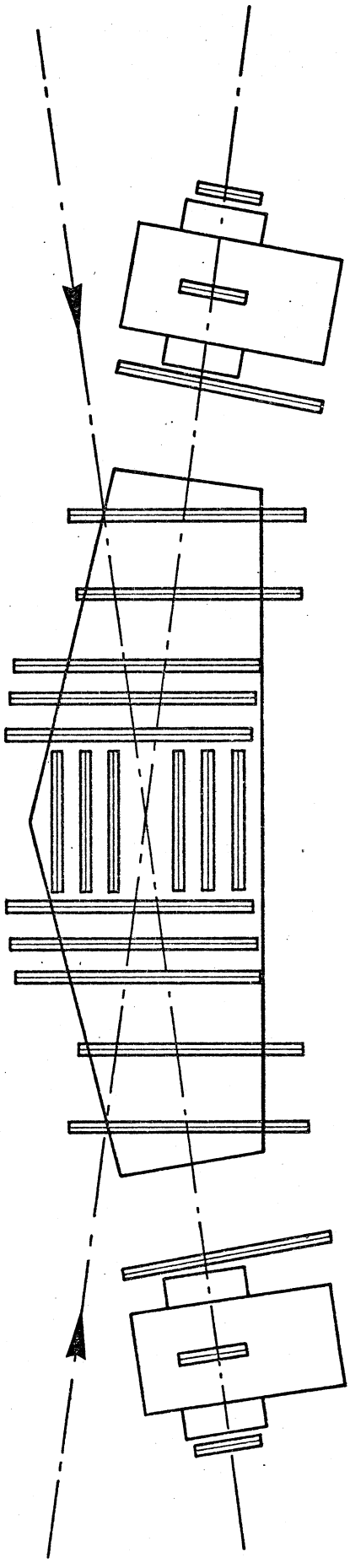

Fig. 3 - Split Field Magnet facility layout.

3) EXPERIMENTAL TECHNIQUE

We intend to measure all the kinematical quantities for the 6-prong events of the type (1). Even relaxing on the energy conservation, which is known to be a weak constraint at ISR, we get a 3C- discrimination against the inelastic background. The need for multiple track detection and large volume momentum analysis strongly suggests the choice of the SFM facility and the related detection system.

In the following we design according to the SFM layout as proposed by CHOV group[18] and shown in fig. 3; the neutron detectors are omitted. The apparatus consists of 22 planes of proportional wire chambers of which the 6 at wide angles will be used to veto the low energy particles, mainly from pionization, whereas the other downstream chambers will detect the high momentum particles. The trigger to be used for this experiment will be described in a later section.

In the calculations we assume a uniform magnetic field of 11 kG in the main magnet an a uniform field of 15 kG in the compensators. The main ISR parametersused in this proposal are given in Table 1.

TABLE 1

beam momentum	25 GeV
crossing beam angle	19°
angular beam spread	0.7 mrad
P_L beam spread	200 MrV/c
P_T beam spread	20 MeV/c
residual gas pressure	10^{-10} torr
doughnut thickness	.15 mm
doughnut thickness	1.2 g/cm^2
luminosity	10^{30} cm^{-2} sec^{-1}

Measurement outline

The trigger will require at least 9 hits in each of the two spectrometer arms, no hit in the wide angle chambers and a maximum of 3 hits per downstream chamber, a "hit" being defined as a recorded intersection of a particle trajectory with the chamber planes. All the events satisfying these requirements will be tape-recorded and computer analyzed. Only a fraction of all triggers will have 3 or more hits for each of the six particles, allowing the determination of their momenta. The first step of the analysis will therefore reject the events in which the momentum measurement is not possible for all the six prongs. The remaining events will give a 3-C fit provided that π^+-p separation is possible.

Fig. 4 and 5 show the π^+ and p momentum distributions of the Montecarlo generated events(*) producing 3 hits per particle in the apparatus; only a small fraction of the π's have momenta higher than 12 GeV/c and only a small fraction of protons have momenta lower than this limit.

As indicated in Table 2, the events having a positive particle with momentum higher than 12 GeV/c and the other positive particle with momentum below this limit are a large fraction of the total. If we assume the particle with higher momentum to be always the proton, the percentage of wrong assignements with respect to the total number of detected events is low and is given in Table 2. This way practically all the events with the proton going forward in the N* C.M.S. are detected. The complete decay angular distribu

(*) Here and in the following, we report only distributions relative to the extreme cases of N*N* production, namely N*(1470)-N*(1470) and N*(2190)N*(2190).

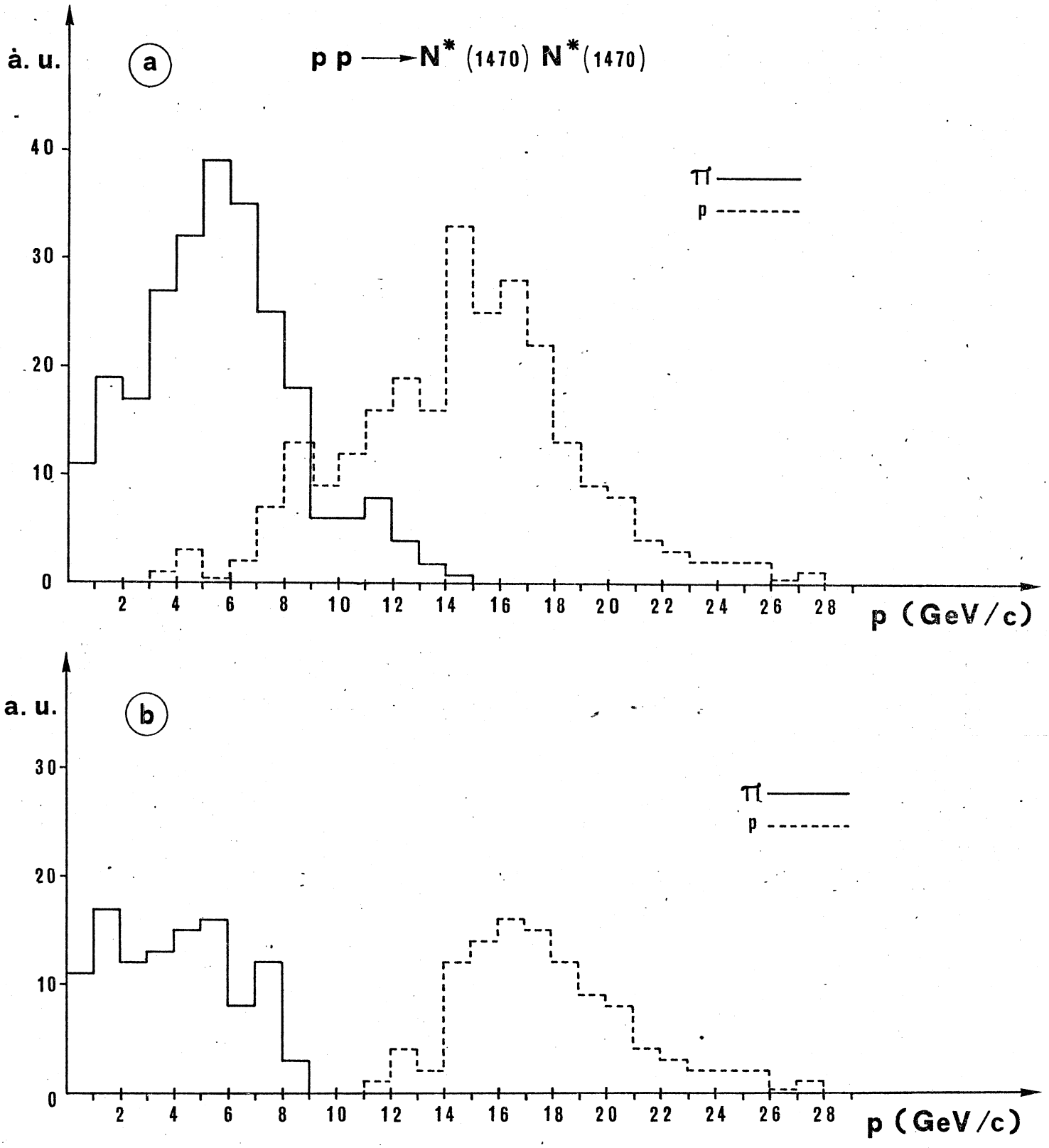

Fig. 4 - Momentum distributions of pions and protons from double N*(1470) production: (a) all detected events (b) detected events with the decay proton in the forward CMS hemisphere.

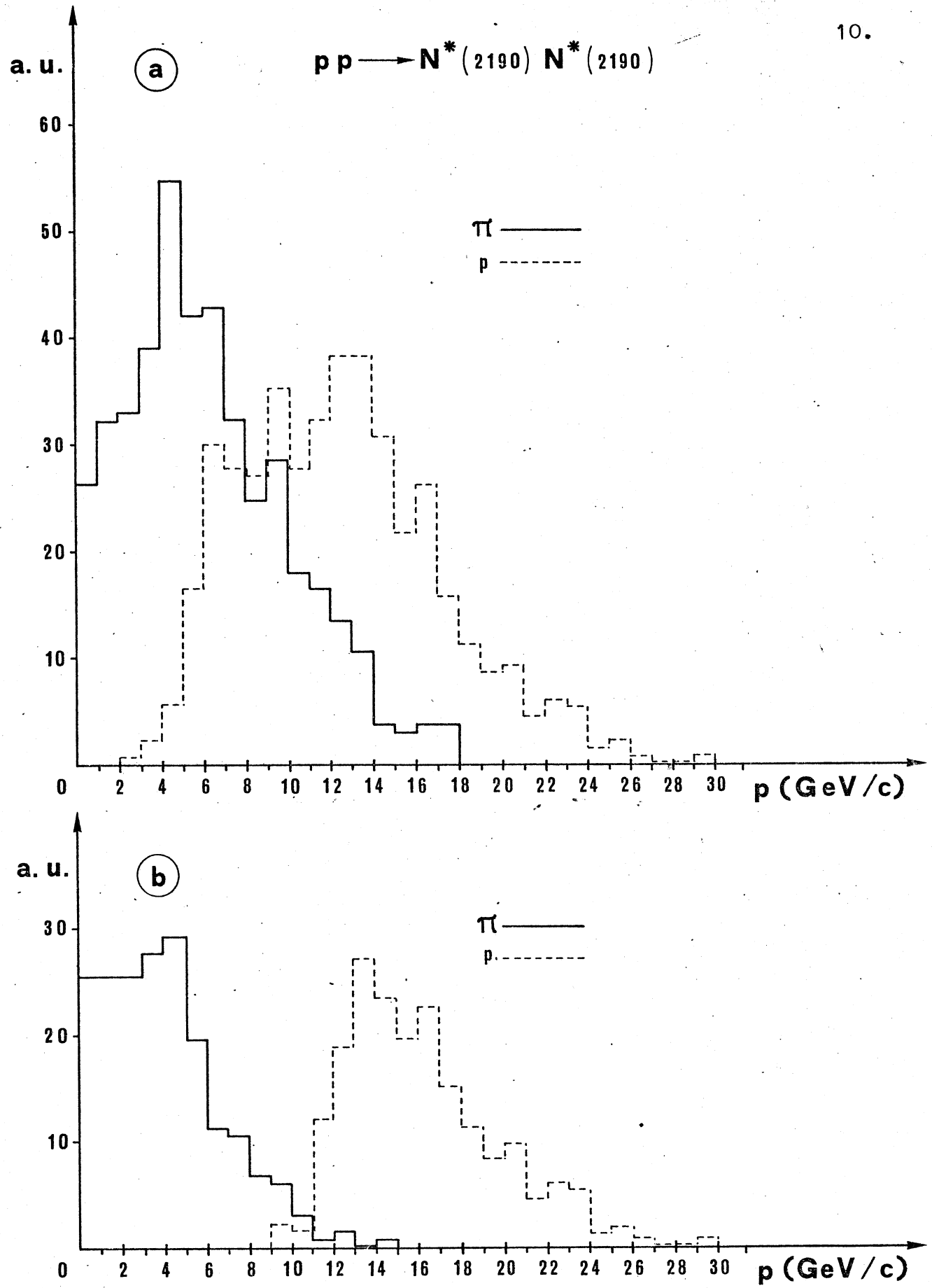

Fig. 5 - Momentum distributions of pions and protons from double N*(2190) production: (a) all detected events
(b) detected events with the decay proton in the forward CMS hemisphere.

TABLE 2

Detected double N* events	N* combinations	
	1470-1470	2190-2190
(1) fraction of the events with the particle having the label "proton" with $p > 12$ GeV/c (see fig. 4a, 5a)	60%	46%
(2) fraction of the decays of (1) with the protons going forward in the N* CMS	98%	85%
(3) fraction of (1) with the π having $p > 12$ GeV/c (wrong assignement).	7.2%	27.4%

tion can be obtained assuming forward-backward symmetry.

In conclusion, the selection of the events of type (2) is possible because of their strong signature and of the high confidence level in the identification of the final state particles. This selection can be further improved taking into account also the angular distributions of Fig. 6, 7 and by means of the kinematical fit.

Monitor

We plan to use the elastic scattering as luminosity monitor. The corresponding trigger will require one charged particle in each arm of the spectrometer at small angles; the most convenient detection region of the apparatus for elastics will be chosen in the test runs where a direct experimental check of the ratio between trigger and background rates will be possible.

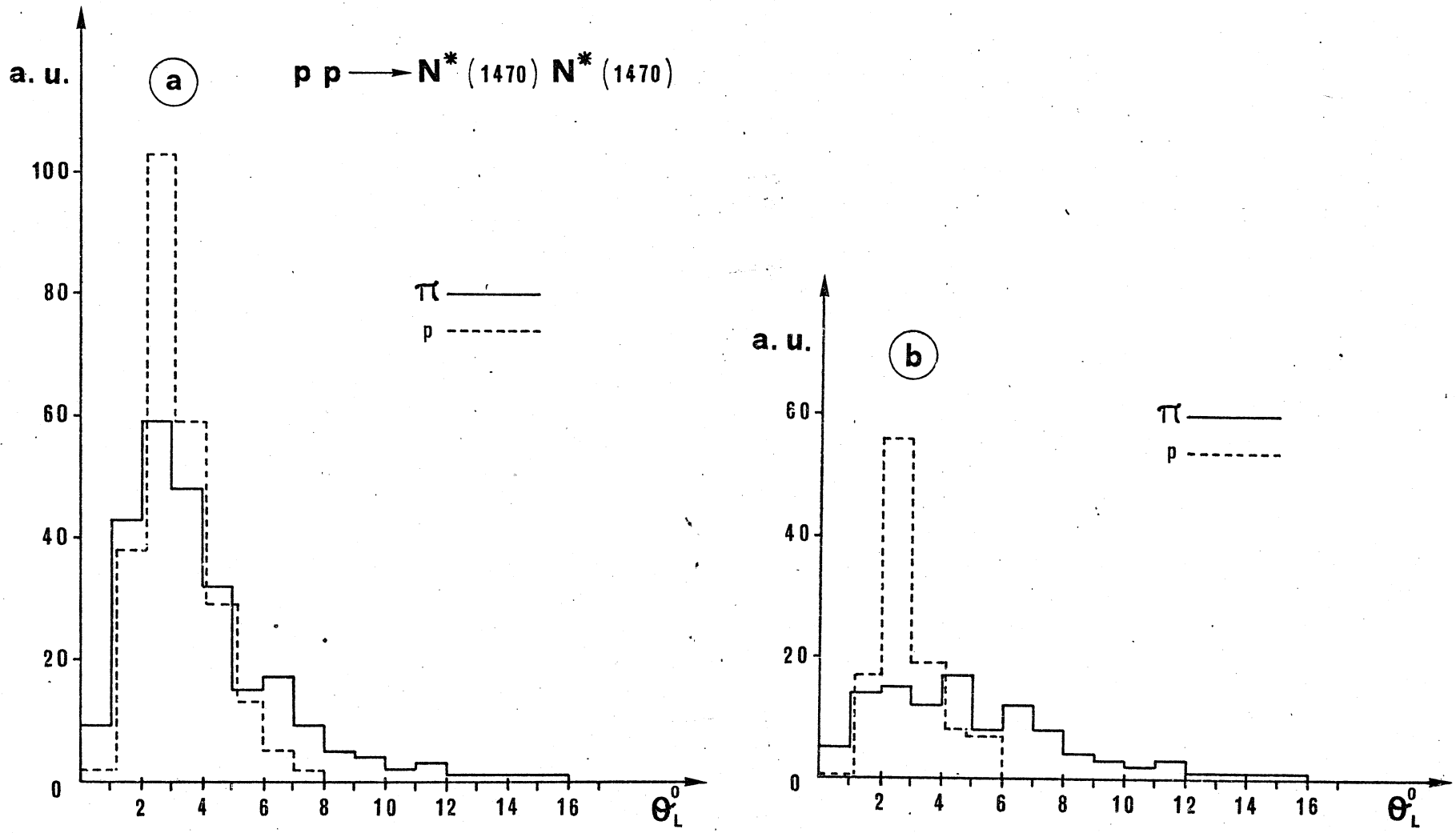

Fig. 6 - Angular distributions with respect to the incident beams of pions and protons from double N*(1470) production:
(a) all detected events
(b) detected events with the decay proton in the forward CMS hemisphere.

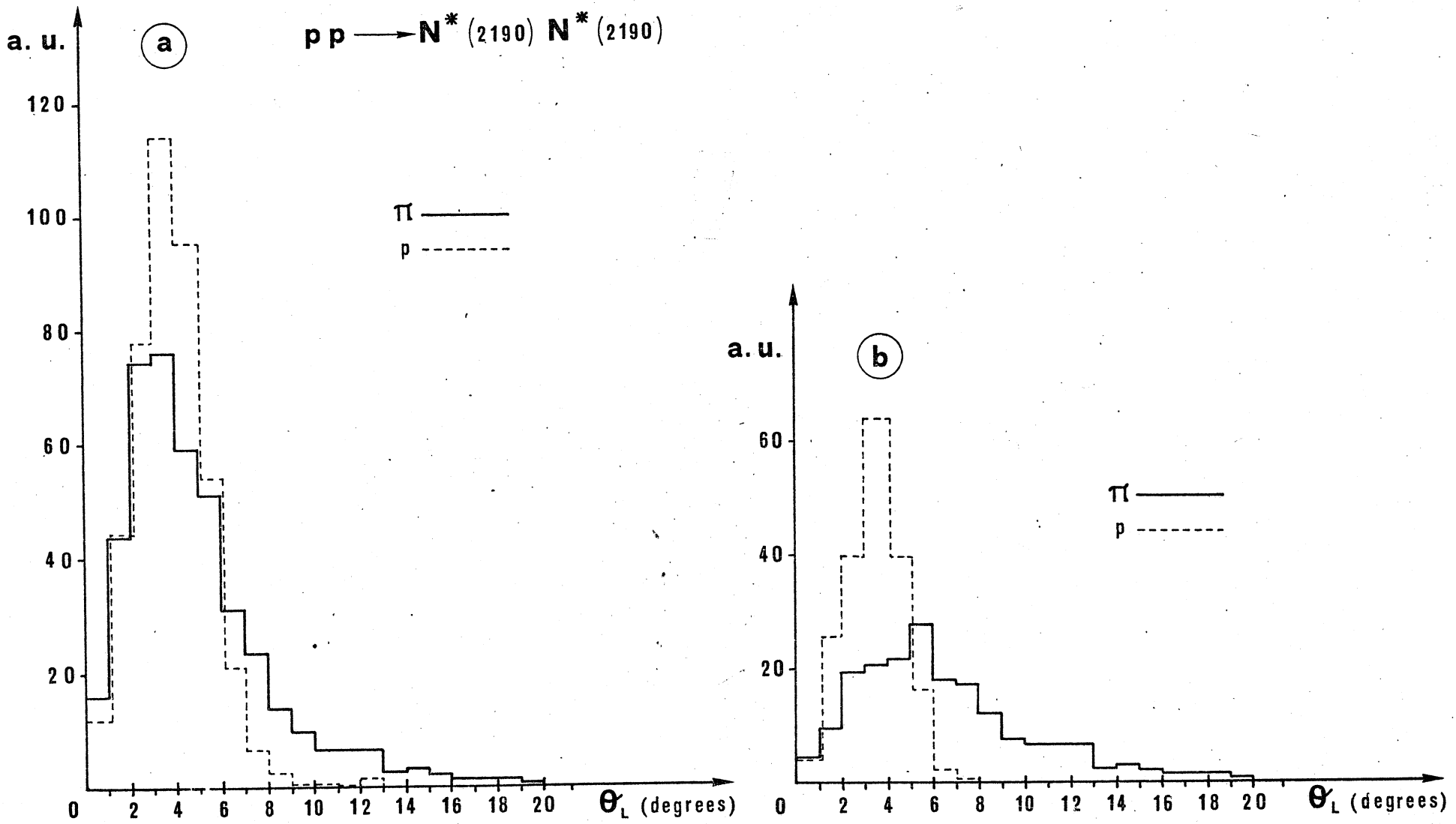

Fig. 7 - Angular distributions with respect to the incident beams of pions and protons from double N*(2190) production:
(a) all detected events
(b) detected events with the decay proton in the forward CMS hemisphere.

4) CROSS-SECTION ESTIMATES

A rough estimate of the total cross-sections for double isobar production can be obtained assuming factorization:

$$(4) \qquad \sigma(N^*_i N^*_j) = \frac{\sigma(pN^*_i)\,\sigma(pN^*_j)}{\sigma(pp)}$$

The experimental values of $\sigma(pN^*)$ at 28 GeV and the extrapolation to 1500 GeV by means of the formula $\sigma = k p_{lab}^{-n}$ are given in Table 3 and 4[19].

TABLE 3

N*(MeV)	1470	1520	1688	2190
σ(28 GeV)	700 μb	170 μb	560 μb	110 μb

With the experimental branching ratios for the decay $N^* \to p\,\pi^+\,\pi^-$

N*(MeV)	1470	1520	1688	2190
$N\pi\pi$	40%	0	10%	70%?
$\Delta\pi$	-	10%	30%	-

and the following probability values obtained from the Clebsh-Gordon coefficients:

$$P\left[N^* \to (N\pi)_{T=1/2}\,\pi \to N\pi\pi\right] = .44$$
$$P\left[N^* \to \Delta\pi \to N\pi\pi\right] = .56$$

we can estimate the branching-ratios for the decay of both N* into $p\,\pi^+\,\pi^-$ (see Table 4).

For the behaviour of the differential cross-section, we assumed a diffraction-like t-dependence similar to the single produc-

tion cross-section:

$$\frac{d\sigma}{dt} = A\ e^{bt}$$

A rough evaluation of the parameters A and b can be phenomenologically achieved applying factorization to the differential cross-sections for single N* production with the following values of b[19]:

PP ⟶	N*(1470)P	N*(1520)P	N*(1688)P	N*(2190)P	PP
$b(GeV/c)^{-2}$	18	4.3	5.5	5.1	9

One obtains for the vertex constant of the process

$$p + p \longrightarrow N^*_i + N^*_j$$

the following relation

$$a_{pN^*_iP} \quad b_{N^*_i}/2 - 2.25$$

where $a_{pN^*_iP}$ represents the proton-N*-Pomeron vertex constant. The obtained values of b are reported in Table 4.

TABLE 4

N*-N* combination	σ (μb) extrapolation to 1500 GeV	Branching Ratios	b(GeV/c)^2
1470-1470	13.5	.03	27
1520-1520	5	.08	0
1680-1680	80.	.05	2
2190-2190	0.2	.1	1.2
1470-1520	8	.05	--
1470-1688	30	.04	14.5
1470-2190	1.5	.06	14
1520-1688	20	.06	--
1520-2190	1	.09	--
1688-2190	3	.07	1.6

The extrapolated errors are not reported in the Table. In the case of the double N*(1680) production, which is the most relevant one, $\sigma(1500\ \text{GeV}) = 80 \pm 57\ \mu b$.

5) DETECTION EFFICIENCY

The detection efficiency of the reaction (2) was evaluated by means of a Montecarlo calculation with the following procedure:

1) a pair of values m_1, m_2 of isobar invariant masses was generated according to the Breit-Wigner formula and the known widths of the various isobars. A two-body reaction $pp \rightarrow m_1 m_2$ was generated according to $\sim e^{bt}$, with b given in Table 4 for each isobar pair.
2) A C.M.S. isotropic decay in the $p\pi^+\pi^-$ -channel was assumed for each isobar, the momentum of each particle being given by

the phase-space distribution. The trajectories of all the 6 particles were then reconstructed in the apparatus.

3) The intersection points of the 6 trajectories with the chamber planes were determined. Events were labelled "detected" according to the criteria described in section 3b).

A total of $\sim 5.10^4$ events were generated for 25 GeV beams momenta and the efficiency ε for each isobar pair is reported in Table 5.

Fig. 8 shows the t-dependence of the detection efficiency for some isobar pairs. No sharp variation of the detection efficiency is present near the minimum attainable t.

TABLE 5

N*-N* combination	$\varepsilon \times 10^3$	σ_{eff}(nb)	$\frac{\varepsilon_{trigger}}{\varepsilon_{eff}}$	$\sigma_{trigger}$(nb)
1470-1470	4.2	1.7	26	44.
1520-1520	6.5	2.6	18	47.
1688-1688	12	48.0	11	528.
2190-2190	28	0.6	5	3
1470-1520	5.3	2.1	23	48
1470-1688	7.2	8.6	17	146
1470-2190	10.9	1.0	11	11
1520-1688	8.9	10.7	15	161
1520-2190	13.5	1.2	10	12
1688-2190	18.4	3.9	7	27
	Total	80.4		1027

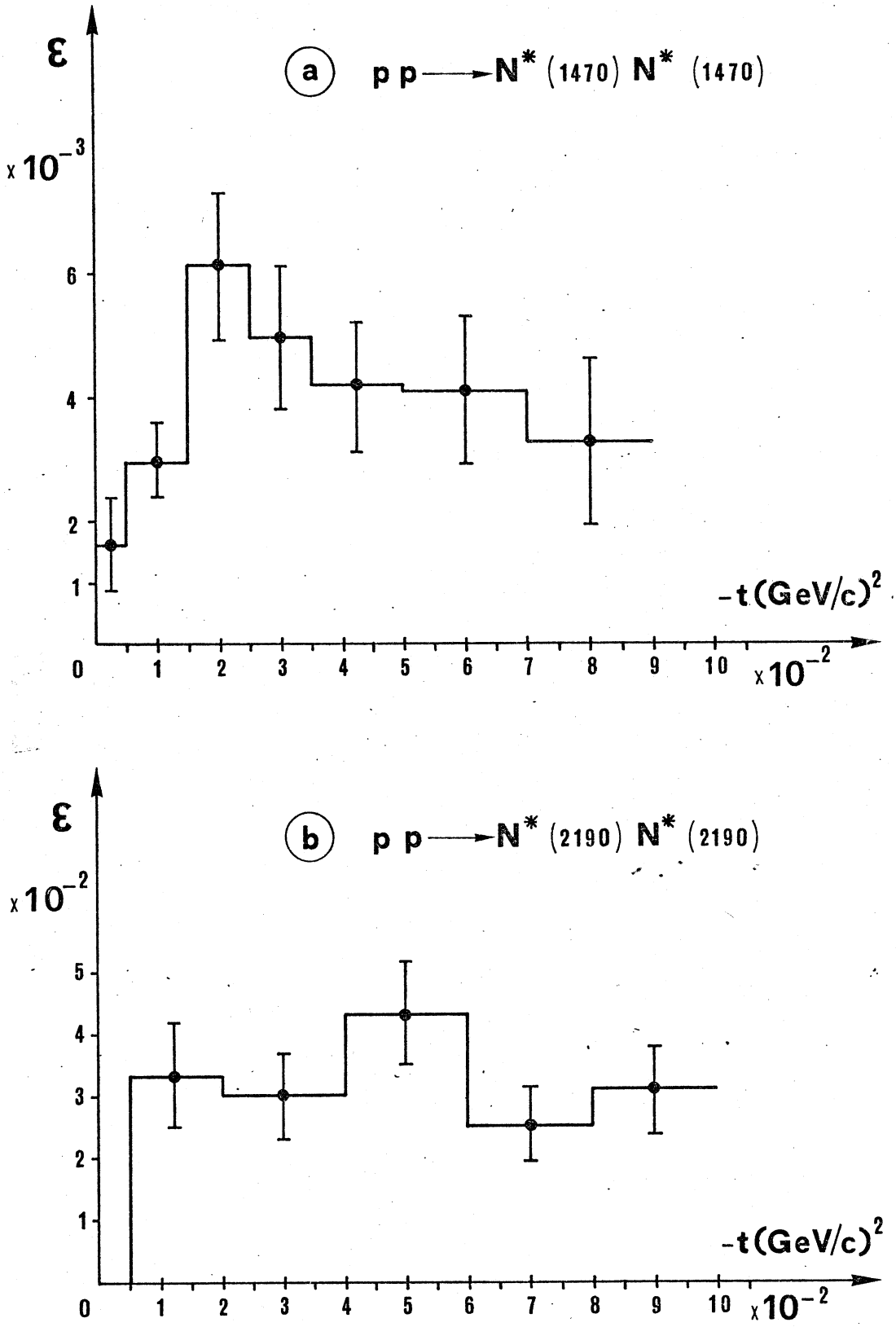

Fig. 8 - t-dependence of the detection efficiency:
(a) p + p ⟶ N*(1470) + N*(1470)
(b) p + p ⟶ N*(2190) + N*(2190)

6) ERRORS AND RESOLUTION

a) Angles and momenta measurement

With a Montecarlo calculation we estimated the errors on the particle angles and momenta, assuming a point error of .6 mm, typical for proportional wire chambers with a least-count of 2 mm. The results are shown in Figgs. 9, 10, 11, 12.
The average error is about 1 mrad for angles and about 2-3% for momenta.

b) Multiple scattering and nuclear interactions

Multiple scattering in the doughnut walls gives rise to a further error on the particle angles determination and therefore on the transverse momenta. The average scattering angle evaluated for a wall thickness of .15 mm is shown in Table 6; typical momenta and angles of π's and protons were assumed (figgs. 4 to 7).

TABLE 6

N*N*	Particle	$\delta\bar{\theta}$ (mrad)	δp_T (MeV/c)	α
1470-1470	π p	1.09 0.46	~6 ~8	9.10^{-2}
2190-2190	π p	1.00 0.47	~5 ~7	6.10^{-2}

The fraction α of the events having at least one particle undergoing nuclear scattering is shown in column 5 of the same Table. The multiple scattering errors are negligible if compared to the angular beam divergence ($\delta\theta \simeq .7$ mrad, $\delta p_T \simeq 20$ MeV/c) and to the measurement errors.

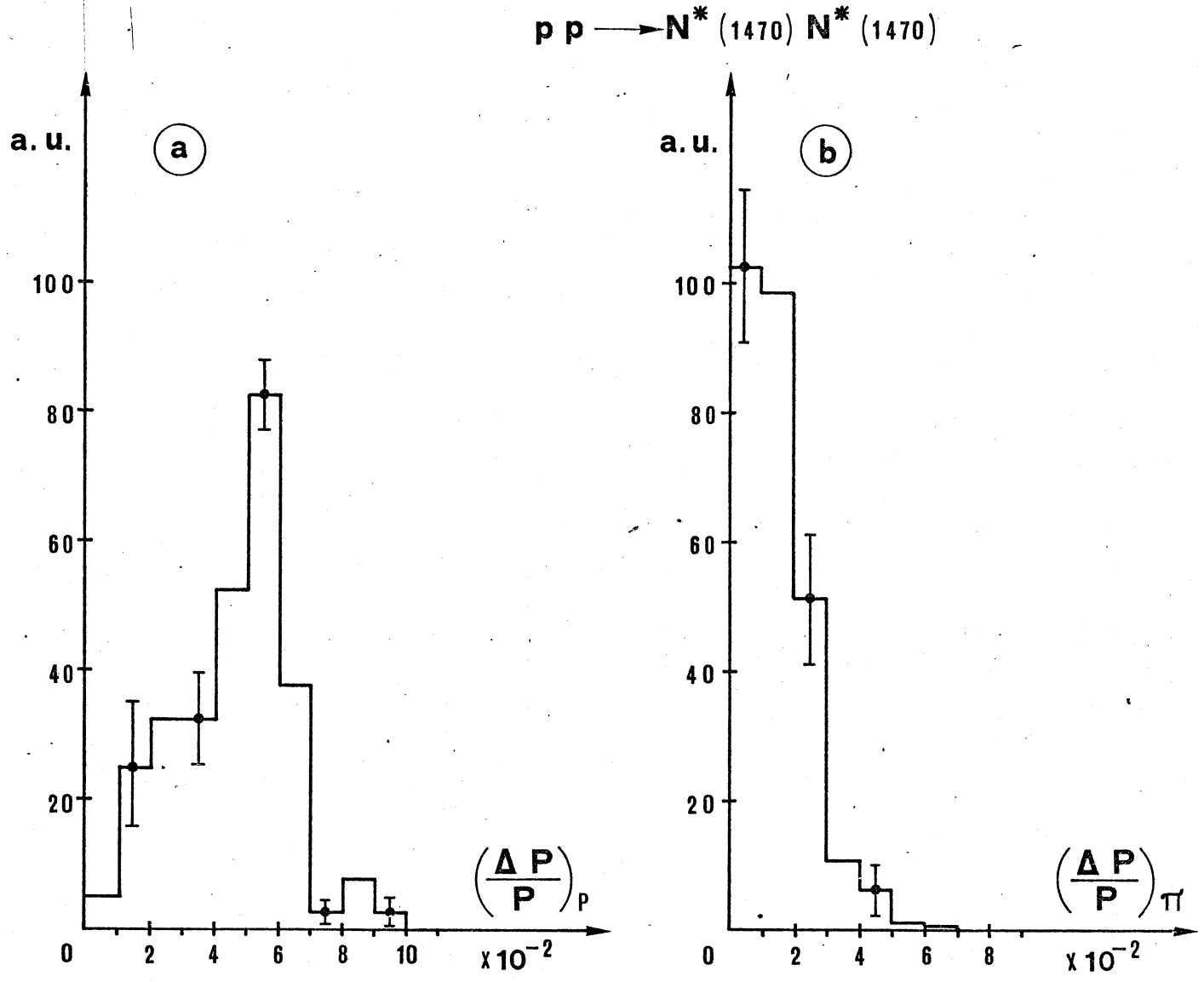

Fig. 9 - $\Delta p/p$ distributions of protons (a) and pions (b) for the reaction p + p ⟶ N*(1470) + N*(1470).

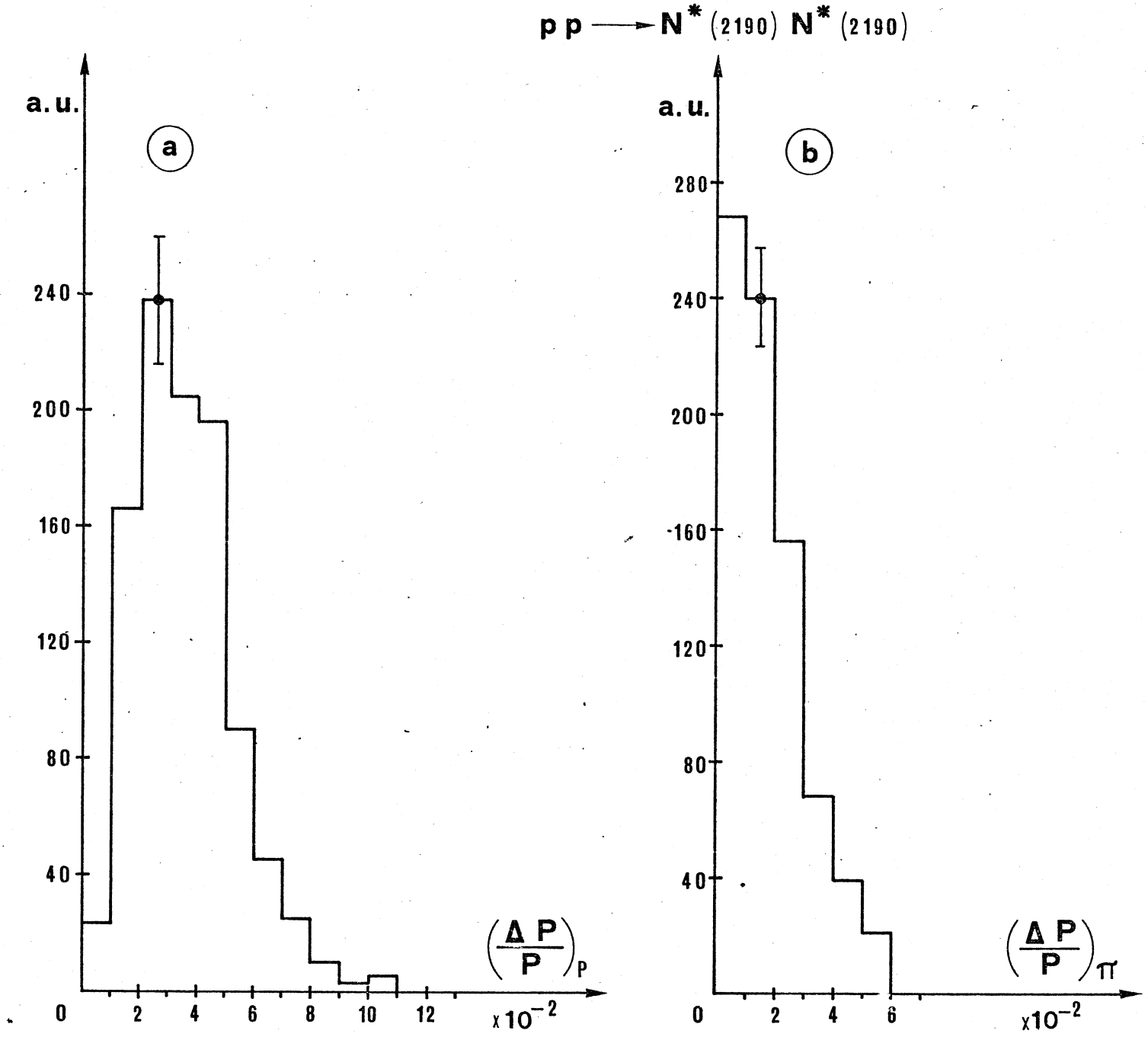

Fig. 10 - $\Delta p/p$ distributions of protons (a) and pions (b) for the reaction p + p ⟶ N*(2190) + N*(2190).

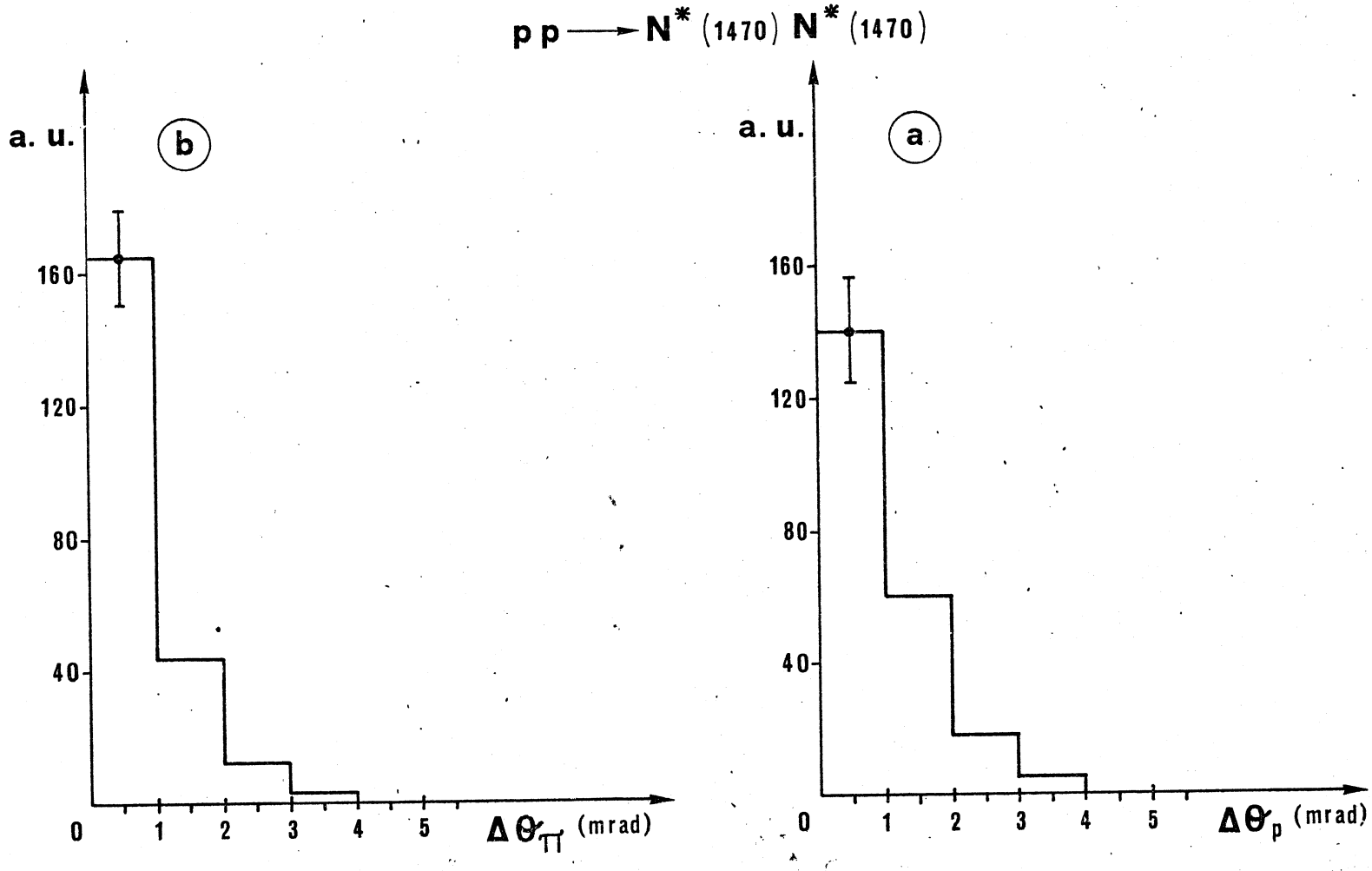

Fig. 11 - $\Delta\theta$ distributions of protons (a) and pions (b) for the reaction p + p ⟶ N*(1470) + N*(1470).

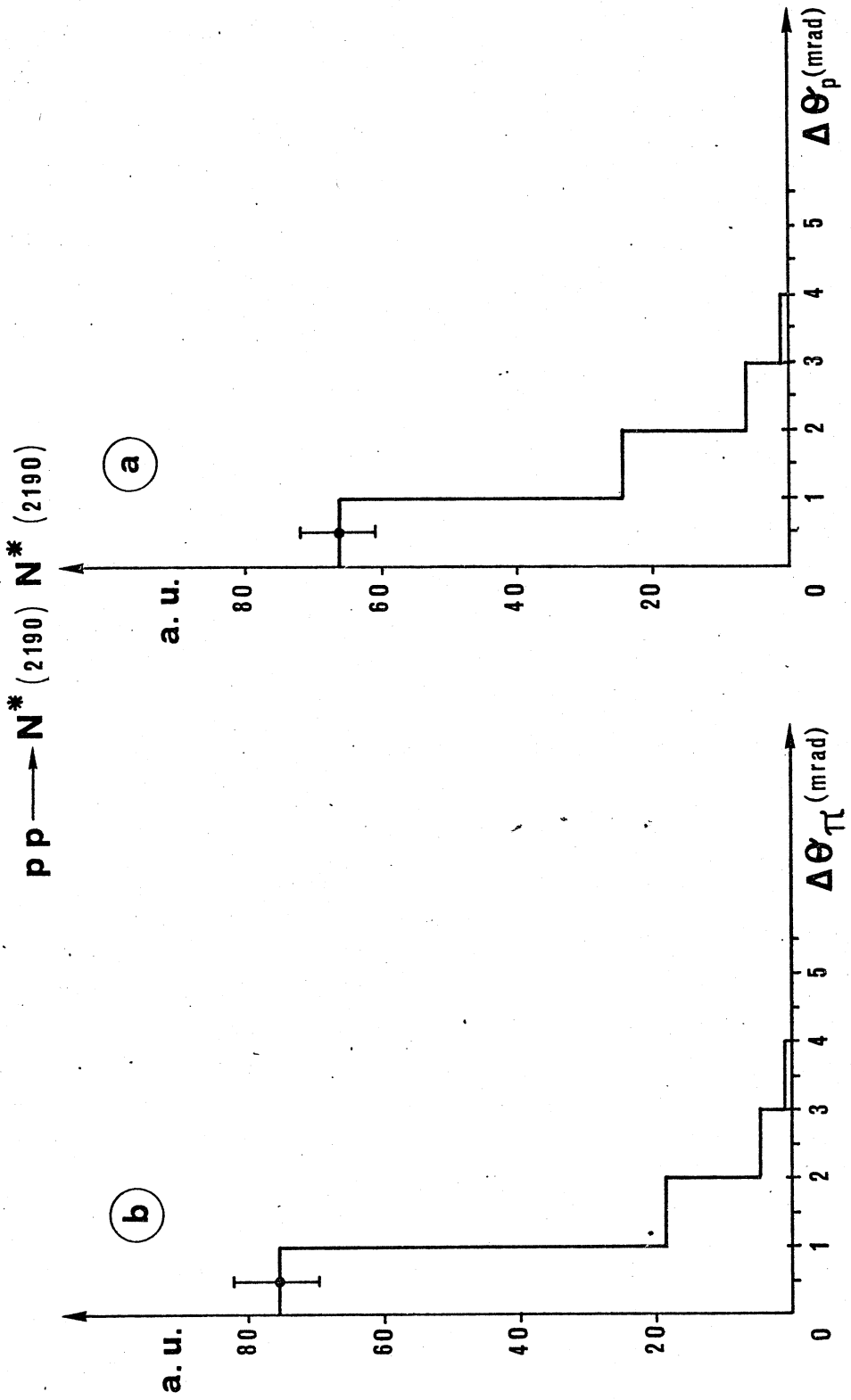

Fig. 12 - $\Delta\theta$ distributions of protons (a) and pions (b) for the reaction p + p ⟶ N*(2190) + N*(2190).

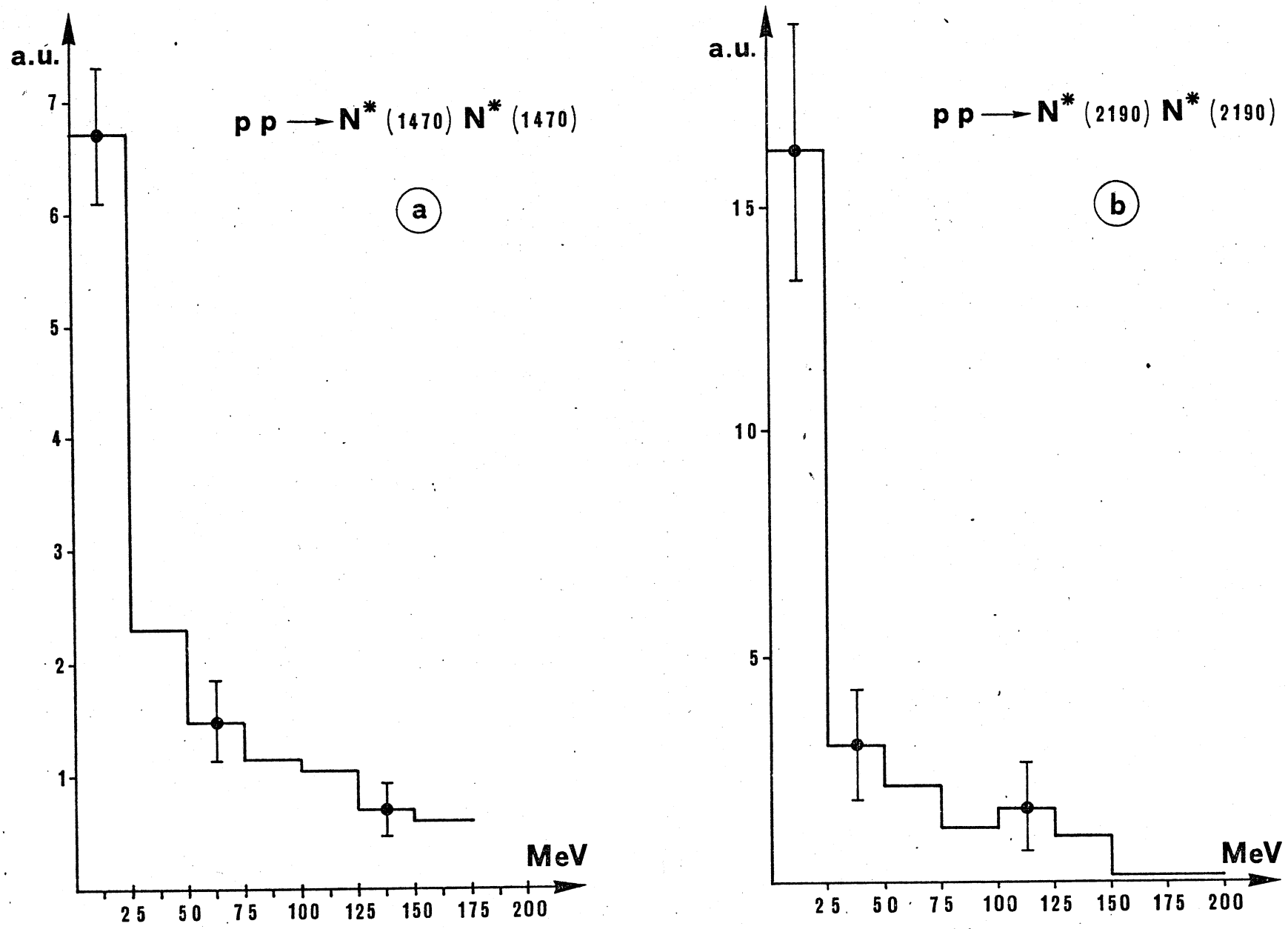

Fig. 13 - Mass resolutions for the reactions:
(a) p + p → N*(1470) + N*(1470)
(b) p + p → N*(2190) + N*(2190)

c) Mass resolution

With the same Montecarlo calculation we reconstructed the masses of the produced isobars, taking into account only the experimental uncertainty on the coordinate measurement. Fig. 13 shows the absolute value distribution of the difference between the reconstructed and the generated masses. The average mass resolution is 25-30 MeV.
The estimated error on the masses due to a beam momentum spread of 200 MeV/c amounts to a few MeV, as shown in Fig. 14.

All these error evaluations do not take into account the kinematical fit: true errors will be lower than the estimated ones.

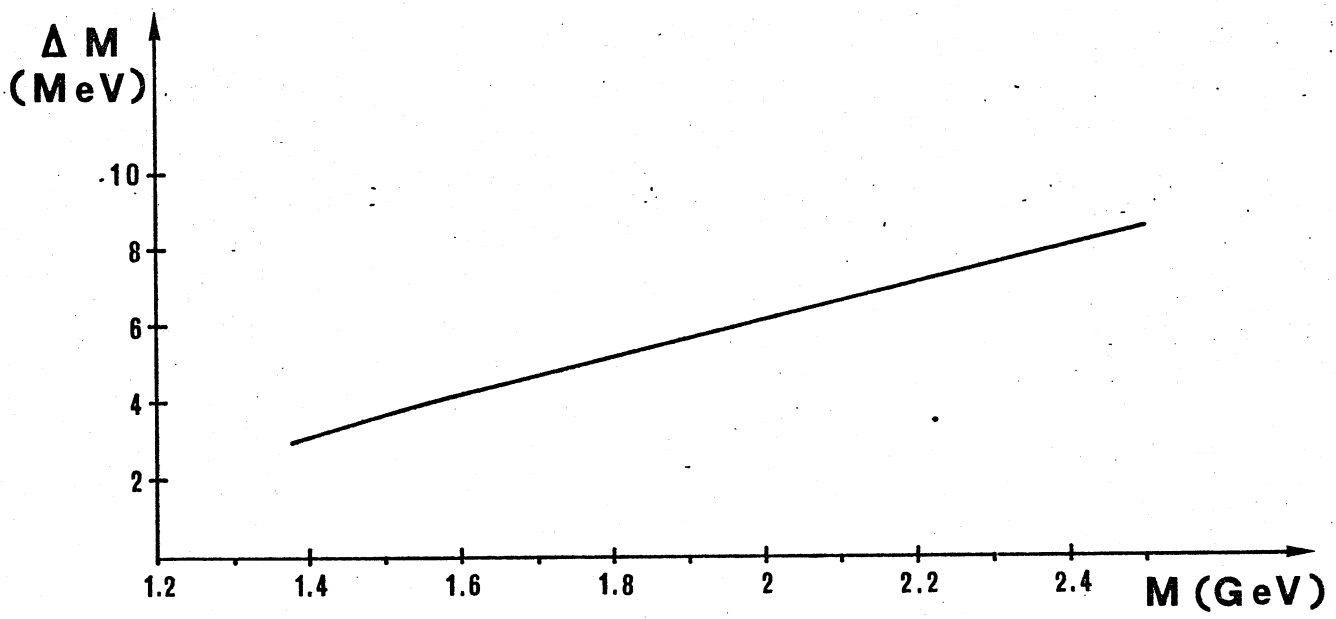

Fig. 14 - Dependence of the contribution to the mass error due to a beam momentum spread of 200 MeV/c on the mass of the produced system.

7) BACKGROUND

The background contributions to the total trigger rate can be roughly divided into three classes: high charged multiplicity events, neutrals in the final state (both originating from beam interactions) and particle production on the residual gas. Although these classes may have common properties, we shall discuss them separately in what follows.

a) High multiplicity events

Assuming energy independence, the total inelastic cross-section amounts to ~ 30 mb at ISR energies and the relative prong probability can be obtained by means of the measured topological cross-sections[20].

The probability that each of these channels fullfills the trigger conditions as described in section 3 was estimated by means of a Montecarlo calculation. Assuming a thermodinamical-isobaric model with momentum distributions obtained from cosmic-ray data[21], we calculated the probability for any number of hits in the detection apparatus for such jet-like events, using for the number of prongs a Poisson distribution with $\bar{n} = 8$[22].

The results, shown in Fig. 15, give for this "trigger efficiency" a value of about 2.10^{-6} obtained by extrapolation to the minimum required number of 18 hits. A subset of these events fullfills also the requirement of having three measurable tracks in each detection arm: this will represent a source of background at the input of the analysis section of the experiment. This fraction of events was estimated by making use of a combinatorial approach considering the probabilities for each track of being measured and vetoed. The effective cross-section for a jet-like reaction

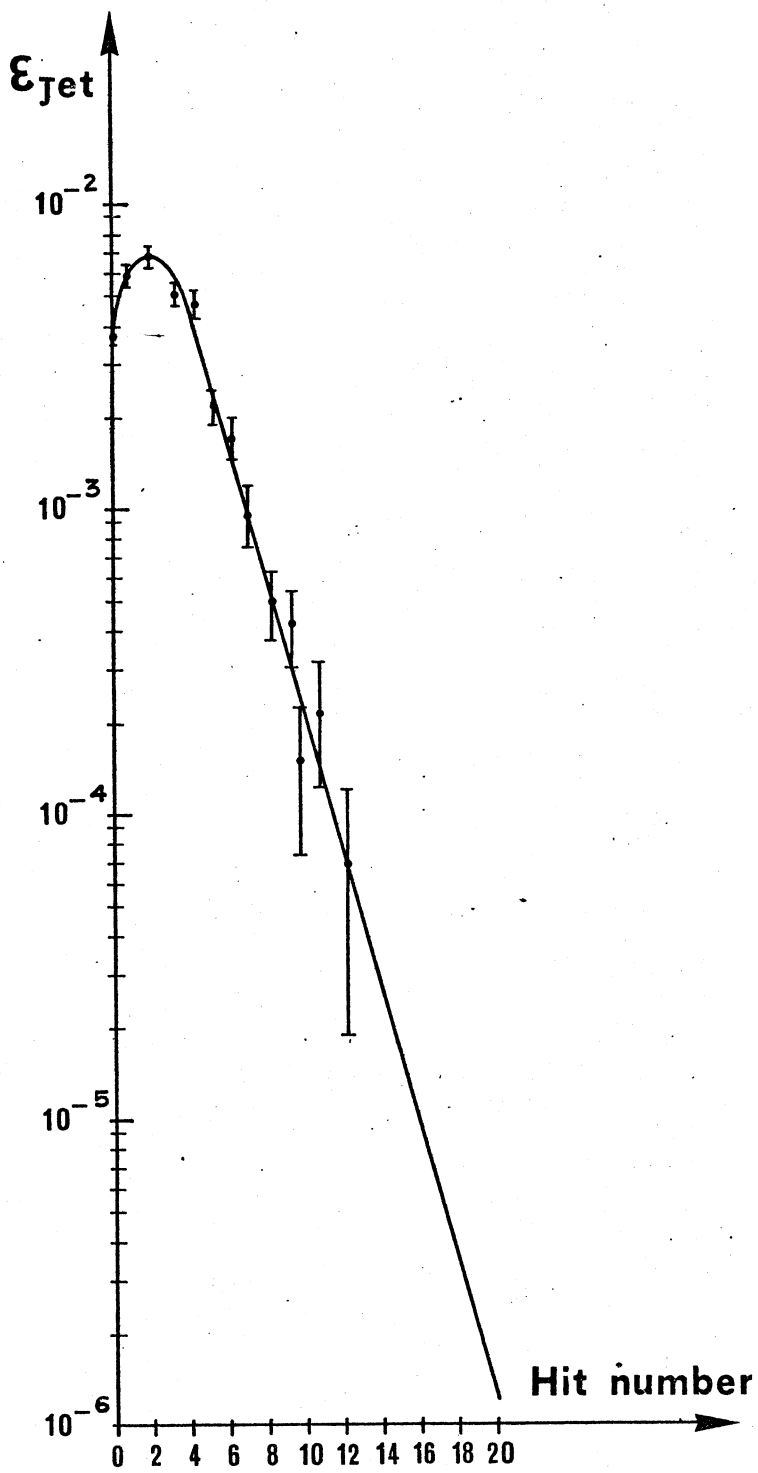

Fig. 15 - Detection efficiency ε_{jet} versus hit number for jet-like background. The extrapolated trigger efficiency to a total of 18 hits amounts to $\sim 2.10^{-6}$.

of any multiplicity to be detected as a fully measurable 6 prongs events is given by:

$$\sigma = \sum_{n=6}^{16} \sigma_n \, X^6 (1-X)^{n-6} \, (1-Y)^{n-6}$$

where σ_n is the topological cross-section for n prongs; X = .09 and Y = .66 are the average probabilities for each track to be measurable and vetoed respectively.

The results are shown in Table 7 where the effective cross-sections at the trigger and at the analysis levels are reported; their ratio is also indicated. The same quantities for the real events are reported for comparison.

TABLE 7

	N*N* production	Backgroung jet-like
$\sigma_{phys.}^{Total}$	80 nb	10 nb
$\sigma_{trigger}^{Total}$	1030 nb	180 nb
$\sigma_{phys.}^{Total} / \sigma_{trigger}^{Total}$	1/13	1/18

b) Neutrals

Neutral contamination of the recorded events can be essentially restricted to a fraction of the reactions having one π^0 in the final state, neutrons and multiple π^0 production being rejected to a very high degree by the requirement of momentum balance.

The only experimental result available to date is a measurement of the total cross-section for the process[23]

(4) $$p + p \rightarrow p + p + 2\pi^+ + 2\pi^- + \pi^0$$

which amounts to about 1.4 mb at 28 GeV. Since the energy dependence is not determined, we make the strong overestimate of assuming this channel cross-section constant in energy. The double N* production at 1500 GeV is estimated with factorization to be about 200 μb and the fraction of the decays $(N\pi^+\pi^-) + (N\pi^+\pi^-\pi^0)$ (which contribute to reaction (4)), detected in the apparatus with an average efficiency of 1%, amounts to only a few nb. The remainingcontribution to reaction (4) can be assumed to be given by jet-like events for which the average detection efficiency is around 10^{-6}. This very rough estimate gives a contamination of single π^0 production to our effective cross-section of less than 10%. A further reduction at this stage is achieved by considering the transverse momentum reconstruction uncertainty which amounts to about 100 MeV/c(*). Assuming the usual transverse momentum distribution(24)

$$\frac{dN_{\pi^0}}{dP_T} \propto P_T\, e^{-P_T(GeV)/.17}$$

the percentage of π^0 with $p \lesssim 100$ MeV/c is about 4%.

c) Beam-gas interactions

Assuming a conservative value of 10^{-10} torr for the residual pressure near the interaction region, we get for 7 A circulating current 0.8×10^{8} $(\frac{\text{nucleon}}{\text{cm}^3})$ x 4×10^{19} $(\frac{\text{proton}}{\text{sec.}})$ x 4×10^{-26} $(\text{cm}^2) \simeq 1.2\,10^{2}$ (interactions/sec.cm).

By using a time of flight tecnique, with two counters positioned at the ends of the main magnet, the effective length for beam-gas triggers is a region about 2 meters long at the end of the last bending magnet. We get 1.2×10^{2} $(\frac{\text{interaction}}{\text{sec.cm}})$ x 4×10^{2} (cm) $\simeq 4.8\times10^{4}$ $(\frac{\text{event}}{\text{sec.}})$ from the two rings, which are easily rejected with a moderate resolution of about 1 nsec to be compared with a time of

(*) - See Appendix

flight basis of $\simeq$ 35 nsec.

The effective rate of beam-gas interactions occurring inside the main magnet volume is about 5×10^4 ev/sec; such interactions should not trigger both time of flight counters thus reducing the contamination to the fast trigger rate to the random level.

In both cases a further reduction of the background due to beam gas interactions is obtained taking into account the veto of the large angle chambers.

8) TRIGGER

On the basis of the logic structure of the main trigger, as described in the previous sections, it is possible to realize a simple logic function which satisfies its basic requirements making use of the fast card signals of the proportional chambers.

This trigger will have the following properties:

1) a fast decision section (typically 100 nsec) as a simple logic combination of signals from time of flight system and the "chamber OR's" from both the transverse and the longitudinal planes. This is to store the information in the wire latches and switch to the subsequent processing.
2) An advanced reject section (typically 200-300 nsec), in case more than three hits are present in any of downstream chambers.
3) A main logic section to check for a minimum of nine hits in both detection arms of the SFM (typically $\lesssim 1\,\mu$sec) and to transfer control to the computer.

We emphasize that by using the card signals for this logic it

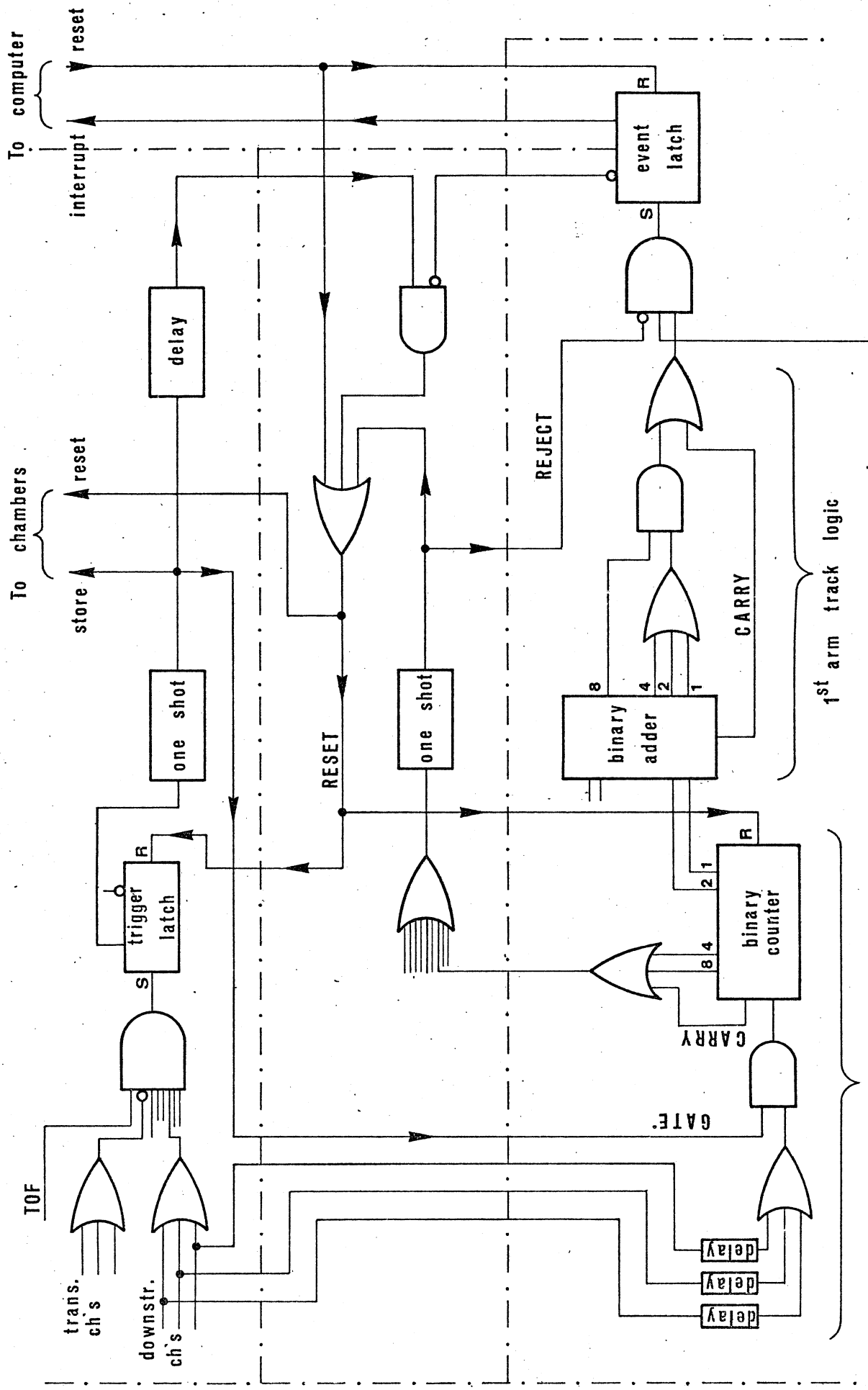

Fig. 16 - General schematic of the trigger logic.

is possible to realize a relatively simple and fast trigger which, to the expense of a negligible amount of phase space, can overcome most of the wire clustering problems and is capable of taking fast decisions at the pattern acceptance stage. A general schematic of the logic is shown in Fig. 16.

A reasonably fast rejection logic is required to handle a maximum interaction rate of about 4×10^4 events/sec at 2x7 A circulating current. Assuming 200 nsec dead-time the upper limit for the non-accepted triggers is

$$R = \left(1 - \frac{1}{1 + 4.10^4 \text{ ev/sec} \times 2.10^{-7} \text{ sec}}\right) \simeq .8\%$$

9) RATES

Table 8 summarizes the expected effective cross-sections and related counting rates, at a luminosity of 10^{30} $cm^{-2} sec^{-1}$.

TABLE 8

effective cross-sections:		
	N* - N* production: trigger	1030 nb
	N* - N* production: analyzable events	80 nb
	background: trigger	180 nb
	background simulating signal topology (to be reduced with momentum conservation)	10 nb
	total trigger	1210 nb
triggers per hour		4350
number of N* - N* events per hour		290

TABLE 9

N*N*	(1) events / 120 h	(2)	(3)	(4)	(5)	(6)	(7)
1470-1470	740	50	690	.60	415	.072	30
1520-1520	1130	80	1050	.59	620	.080	50
1680-1680	20810	1460	19350	.56	10835	.120	1300
2190-2190	265	20	245	.46	115	.274	30
1470-1520	920	65	855	.60	515	.076	40
1470-1680	3765	265	3500	.58	2030	.096	195
1470-2190	440	30	410	.53	215	.173	35
1520-1680	4680	320	4355	.57	2480	.100	25
1520-2190	545	40	505	.52	265	.177	45
1680-2190	1705	120	1585	.51	810	.197	160
Total	35000	2460	32545	-	18300	-	1910

(1) produced N*N* events in 120 h at a luminosity of 10^{30} cm^{-2} sec^{-1}

(2) events not reconstructed because of nuclear scattering (upper limit)

(3) total reconstructed events

(4) fraction of reconstructed events labelling "proton" the particles with p 12 GeV/c

(5) reconstructed events with the above π^+-p identification

(6) fraction of the events of column (5) with wrong $^+$-p assignement (upper limit)

(7) events with wrong $^+$-p assignement

In 120 hours of running time we can collect a statistics of about 3.5×10^4 fully reconstructed N*N* events at the present luminosity of the machine. In Table 9 the total statistics is distributed among the expected number of events for each combination of different isobars, for those which suffered at least a nuclear interaction and those having a wrong π^+-p identification.

Any eventual increase of the luminosity value will not affect the feasibility of the experiment but proportionally increase the yield of data because the trigger we choose is not rate limited. On the other hand an average luminosity of a factor 3 or 4 lower than the value we used will still correspond to about 10^4 collected events.

We think that $\sim$ 60 hours of test run can be adequate for a total of about 200 hours; in our opinion only a fraction of these hours has to be prime time.

10) LOGISTICS AND PARTICIPATION

All the experimental apparatus we require, with the exception of the fast trigger, is already in existence or in construction for an approved experiment at ISR. We do not require any modification of the actual system and minor variations of its original design will not affect the feasibility of the experiment.

This, toghether with the small amount of running time required, would make the switch to or from our experiment very easy. If necessary, at least part of the running time may overlap a compatible experiment in a parallel mode of data taking.

The monitor reaction will be the small angle elastic scattering.

We plan to use the same arrangement as proposed in[18]. This also is clearly compatible with the simultaneous running possibility outlined above.

The collaboration consists actually of 12 physicists from Pavia and 2 from Princeton. The members of the group have already gained experience in experiments with storage rings, hadron physics with proportional wire chambers and multibody hadronic interactions analysis. Although we don't anticipate manpower problems we are very open to participation of CERN members interested in this experiment and in SFM utilization.

Further developments of this proposal are planned to improve the present results on particle indentification, kinematical reconstruction and event selection criteria, as well as more complete definition of the experimental details.

APPENDIX

To evaluate the uncertainty of the total transverse momentum reconstruction the following average values for the decay particles are used (see figgs. 4-7, 9-12 referring to Montecarlo distributions):

	2xN*(1470)	2xN*(2190)
proton momentum	17 GeV/c	15 GeV/c
pion momentum	5 GeV/c	4 GeV/c
proton angle	2.5°	3.5°
pion angle	4°	6°
$(\Delta p/p)_p$	4.5%	4%
$(\Delta p/p)_\pi$	1.5%	2%
$\delta\theta_p$	1 mr	1.2 mr
$\delta\theta_\pi$	.7 mr	1 mr

The transverse momentum error can be evaluated for pions and protons with the formula:

$$\delta p_\perp = \delta p \sin\theta + p \cos\theta \, \delta\theta$$

The results are summarized in the following table:

channel	$\delta p_\perp$ (proton)	$\delta p_\perp$ (pion)	$\delta p_\perp$ (total)
N*(1470) + N*(1470)	70 MeV/c	15 MeV/c	105 MeV/c
N*(2190) + N*(2190)	60 MeV/c	20 MeV/c	95 MeV/c

REFERENCES

(1) - A.P. Colleraine, U. Nauenberg: Phys. Revue 161, 1387 (1967)

(2) - G. Alexander, O. Benary, G. Czapek, B. Haber, N. Kidrou, B. Reuter, A. Shapira, E. Simopoulou, G. Yekutieli: Phys. Revue 154, 1284 (1966)

(3) - C. Caso, F. Conte, G. Tomasini, L. Casè, L. Mosca, S. Ratti, L. Tallone-Lombardi, I. Bloodworth, L. Lyons, A. Norton: Nuovo Cimento 55A, 66 (1968)

(4) - S.P. Almeida, J.G. Rushbrooke, J.H. Scharenguirel, M. Behrens, V. Blobel, I. Borecka, H.C. Dehne, J. Diaz, G. Knies, A. Schmitt, K. Strömer, W.P. Swanson: Phys. Revue 174, 1638 (1968)

(5) - Z.S. Takibaev, E.G. Boos, L.A. San'ko, T. Temiraliev, M.G. Antonova, D.L. Ermilova, T.I. Mukhordova, A.V. Kholmetskaya, V.V. Fedoseenko: Sov. Journ. Nucl. Phys. 13, 64 (1971)

(6) - H.O. Cohn, R.D. Mc Culloch, W.M. Bugg, G.T. Condo: Phys. Letters 26B, 598 (1968)

(7) - S.P. Almeida, H.W. Atherton, T.A. Byer, P.J. Dornan, A.G. Forson, J.H. Scharenguirel, D.M. Sendall, B.A. Westwood: Phys. Letters 14, 240 (1965)

(8) - D.R.O. Morrison: Phys. Revue 165, 1699 (1968)

(9) - J.G. Rushbrooke: Phys. Revue 177, 2357 (1969)

(10) - H. Satz: Phys. Letters 29B, 38 (1969); see also: H. Böggild, K. Hansen, H. Johnstadt, R. Möllerud, M. Suk, L. Veje, M. Korkea-Aho, K.V. Laurikainen, P.K. Laurikainen, V. Bakken, S. Bjastad, F.O. Breivik, T. Jacobsen, S.O. Sorensen, O. Danielsson, G.Ekspong, L. Grantström, B. Ronne: Phys. Letters 30B, 369 (1969)

(11) - H. Böggild, E. Dahl-Jensen, K.M. Hansen, H. Johnstad, R. Möllerud, M. Suk, L. Veje, M. Kaartinen, S. Ljung, V. Bakken, S. Bjastad, T. Jacobsen, S.O. Sörensen, O. Danielsson, G. Ekspong, L. Granström, S.O. Halmgren, B. E. Ronne, N.K. Yamdagui: Nucl. Phys. B32, 119 (1971)

(12) - D. Dekkers, J.A. Geibel, R. Mermod, G. Weber, T.R. Willitts, K. Winter, B. Jordan, M. Vivargent, N.M. King, E.J.N. Wilson: Phys. Revue 137, B962 (1965)

(13) - G. Neuhofer, M. Regler, W. Schmidt-Parzefall, K. Winter, G. Flügge, F. Niebergall, K.R. Shubert, P. Schumacher, J.J. Aubert, C. Broll, G. Coignet, J. Favier, L. Massonet, D. Smith, M. Vivargent, W. Bartl, H. Dibon, Ch. Gottfried, J. Penzias, M. Stener: CHOV/7104/KS

(14) - F.J. Gilman, J. Puruplin, A. Schwimmer, L. Stodolsky: Phys. Letters 31B, 387 (1970)

(15) - G. Cohen-Tannoudji, J.M. Drouffe, P. Moussa, R. Peschausk: Phys. Letters 33B, 183 (1970)

(16) - G. Bellettini, G. Cocconi, A.N. Diddens, E. Lillethun, J.P. Scanlon, A.M. Shapiro, A.M. Wetherell: Phys. Letters 18, 167 (1965)

(17) - G. Cocconi, E. Lillethun, J.P. Scanlon, C.A. Stahlbrandt, C. C. Ting, J. Walters, A.M. Wetherell: Phys. Letters 8, 134 (1964)

(18) - C. Broll: CERN memorandum, 21/7/1971, CERN ISRC/69-14, addendum Oct. 1971

(19) - E.W. Anderson, E.J. Bleser, H.R. Blieden, G.B. Collins, D. Garelick, J. Menes, F. Turkot, D. Birnbaum, R.M. Edelstein, N.C. Hien, T.J. Mc Mahon, J.F. Mucci, J.S. Russ: Phys. Rev. Letters 25, 699 (1970)

(20) - W. Kittel: CERN D.Ph. II/Phys. 71-28

(21) - J.M. Kidd: High Energy Physics 2, 265, A.P. 1967)

(22) - L.W. Jones, A.E. Bussiau, G.D. De Meester, B.W. Loo, D.E. Lyon, P.V. Ramana Murthy, R.F. Roth, J.G. Learned, F. E. Mills, D.D. Reeder, K.N. Ericson, B. Cork: Phys. Letters 25, 1679 (1970)

(23) - CERN-HERA 70-2

(24) - G. Neuhofer, F. Niebergall, J. Penzias, M. Regler, K.R. Shubert, P.E. Shumacher, W. Schmidt-Parzefall, K. Winter: Phys. Letter 37B, 438 (1971)